Title
Influence of moisturizer and relative humidity on human emissions of fluorescent biological aerosol particles

Authors
Zhou, Jin
Fang, Wenjuan
Cao, Qingliang
et al.

Publication Date
2016-10-01

DOI
10.1111/ina.12349

Data Availability
The data associated with this publication are in the supplemental files.

Peer reviewed

Influence of Moisturizer and Relative Humidity on Human Emissions of Fluorescent Biological Aerosol Particles

Jin Zhou[1,2], Wenjuan Fang[1], Qingliang Cao[1], Linyan Yang[3,4], Victor W.-C. Chang[1,2,4,*], and William W Nazaroff[2,5]
[1] School of Civil and Environmental Engineering, Nanyang Technological University, Singapore 639798
[2] Berkeley Education Alliance for Research in Singapore, Singapore 138602
[3] Interdisciplinary Graduate School, Nanyang Technological University, Singapore 639798
[4] Nanyang Environment and Water Research Institute, Nanyang Technological University, Singapore 637141
[5] Department of Civil and Environmental Engineering, University of California, Berkeley, California 94720-1710, USA

[*] Corresponding author. Email address: wcchang@ntu.edu.sg

Keywords: WIBS, Fluorescence, Skin, Occupancy, Source strength, Particle shape

Abstract

Utilizing the ultraviolet-light induced fluorescence (UV-LIF) measurement technique as embodied in the Waveband-Integrated Bioaerosol Sensor (WIBS-4A), we evaluated the fluorescent particle emissions associated with human shedding while walking in a chamber. The mean emission rates of supermicron (1-10 μm) fluorescent particles was in the range 6.8-7.5 million particles per person-h (~ 0.3 mg per person-h) across three participants, for conditions when the relative humidity was 60-70% and no moisturizer was applied after showering. The fluorescent particles displayed a lognormal distribution with the geometric mean diameter in the range 2.5-4 μm and exhibited asymmetry factors that increased with particle size. Use of moisturizer was associated with changes in number and mass emission rates, size distribution and particle shape. Emission rates were lower when the relative humidity was reduced, but these differences were not statistically significant.

Practical Implications

The frictional interaction between human skin and clothing has been demonstrated to be a source of aerosol particle emissions from humans. The intensity of the friction is subject to the skin condition, which may be influenced by the use of moisturizers and by the relative humidity of air. This study examined the influence of these two factors on fluorescent bioaerosol emission rates associated with human shedding and found that both factors affected the emission spectrum, in ways that were unexpected in some respects. The experimental protocol undertaken here can be applied to more participants, including investigations of the impacts from the fabric material and clothing with preloaded particles in future work. The results contribute to an improved understanding of bioaerosol emissions from human occupants of indoor environments.

1. Introduction

As summarized in a recent review (Nazaroff, 2016), there are many reasons to be interested in indoor bioaerosols: i) humans spend most of their time indoors and bioaerosols are abundant in the built environment, ii) bioaerosols play important roles influencing public health, and iii) the goal of improving bioaerosol management can influence building operation strategies. Quantification of bioaerosol concentrations and the influencing processes is valuable for multiple applications within the indoor environmental sciences.

Several recent studies have employed DNA-based approaches to examine airborne biological particles in offices, chambers, classrooms and childcare centres (Adams et al., 2015; Hewitt et al., 2012; Hospodsky et al., 2012; Hospodsky et al., 2015; Meadow et al., 2014; Qian et al., 2012; Shin et al., 2015; Yamamoto et al., 2015). These studies have revealed that human occupancy and activities increase the abundance of bioaerosols and also leave human-associated taxa in the built environment. The research of Adams et al. (2015) and Meadow et al. (2014) indicates that

the relative significance of human contributions is subject to many factors, e.g. the mode and rate of ventilation, the temporal pattern of occupancy, and the efficiency of building filters.

The ultraviolet-light induced fluorescence (UV-LIF) measurement technique, embodied in the Ultraviolet Aerodynamic Particle Sizer (UV-APS), has been employed to characterize fluorescent biological aerosol particle (FBAP) levels and occupant emissions indoors: in a controlled chamber (Bhangar et al., 2016) and in a classroom (Bhangar et al., 2014). Handorean et al. (2015) have coupled the Waveband-Integrated Bioaerosol Sensor (WIBS), another embodiment of the UV-LIF technique, with a DNA-based approach, to characterize the proximal bioaerosols associated with hospital textile handling. Compared to DNA-based methods, the UV-LIF technique has the capability to resolve short-term dynamic processes influencing indoor bioaerosol levels.

Healy et al. (2012a) have compared the measurement capabilities of the WIBS and the UV-APS. Overall, that study reported a good correlation between the two monitors. In comparison with the UV-APS, the WIBS offers two advantages: (a) the capability to report fluorescent measurements in three channels because of a 2×2 excitation-emission matrix; and (b) the provision of information about particle shape through the use of spatially resolved optical detection. Further technical description of the WIBS instrument as applied in this study is provided in §2.2.

Previous environmental studies using the WIBS have been conducted in the laboratory (Healy et al., 2012a; Healy et al., 2012b; Toprak and Schnaiter, 2013) and in outdoor air (Crawford et al., 2014; Gabey et al., 2010; Gabey et al., 2013; Healy et al., 2014; O'Connor et al., 2015a; O'Connor et al., 2015b; Perring et al., 2015; Whitehead et al., 2010). The results indicate that airborne spores, bacteria, pollen, and their fragments are detected by the WIBS.

It is worthwhile to note that the WIBS possesses similar limitations as the UV-APS owing to the inherent limitations of the UV-LIF approach to detecting bioaerosols. In brief, some particulate matter of biological origin may not fluoresce and some abiotic particles may be fluorescent. In their studies of outdoor air utilizing the UV-APS, Huffman et al. (2010) and Pöhlker et al. (2012) have suggested that the fluorescent particle levels represent a lower-limit estimate of the abundance of primary biological aerosol particles. Another well-recognized limitation of UV-LIF methods is its lack of specificity. In their chamber studies to catalogue the fluorescence emissions along with the optical particle size of the bioaerosol cultures, Healy et al. (2012b) and Hernandez et al. (2016) suggested that the WIBS could support discrimination between broad bioaerosol categories (pollen, fungi, and bacteria); however, it cannot provide information at level of genus or specie as can DNA-based analysis methods.

Previous research has demonstrated that the frictional interaction between human skin and clothing is an important source of fluorescent biological coarse particles in the diameter range 2.5-10 μm (Bhangar et al., 2016). It is reasonable to expect that the intensity and consequences of such friction should be influenced by skin condition, which may be affected by the use of skin moisturizers and by the relative humidity (RH) of indoor air. In one of the few closely related studies, Hall et al. (1986) reported that the application of skin lotion after showering greatly reduced the number of bacteria and skin scales dispersed from human subjects. However, this study utilized a culture-based analysis method, which can only capture a small subset of bioaerosols. Studies in dermatology (Rawlings and Harding, 2004; Harding et al., 2000) and epidemiology (Su and Guo, 2007) have related dry skin symptoms to low RH conditions, but the subsequent influence on the shedding of skin flakes has not been investigated. Bhangar et al. (2016) reported enhanced emissions of fluorescent particles from human subjects under elevated

RH conditions. But their findings were based on a limited investigation of this parameter. In addition, that study did not differentiate between emissions from the human body envelope and the influence of particles resuspended from carpeting when investigating the influence of RH.

The design of the present study emerged from the context summarized above. Specifically, i) limited studies have reported on fluorescent particle measurements in the built environment utilizing the WIBS; and ii) the influence of moisturizer use and indoor air RH on bioaerosol emissions from occupants are not well characterized. To contribute new knowledge in these research gaps, we undertook a set of experiments in a chamber utilizing the WIBS to characterize bioaerosol emission rates associated with human shedding. To evaluate the effect of moisturizer use and indoor air RH, each of three volunteer occupants followed scripted behavior and the chamber RH was manipulated to target levels. This work is focused on characterizing emissions from the human body envelope, and consequently measures were taken to minimize the influence of particle resuspension from the floor.

2. Methods

2.1 Experimental design and sampling

A small office room on the first floor of a university building was selected as the experimental site. The room configuration is shown in Figure 1. The room has vinyl flooring and is furnished with one metal cabinet, one wooden table, one metal table, and one plastic chair. The room volume was assessed as 39.5 m^3 based on physical dimensions (length × width × height = 4.76 m × 3.10 m × 2.68 m). It has one door leading to an internal hallway and two inoperable windows mounted high on two walls.

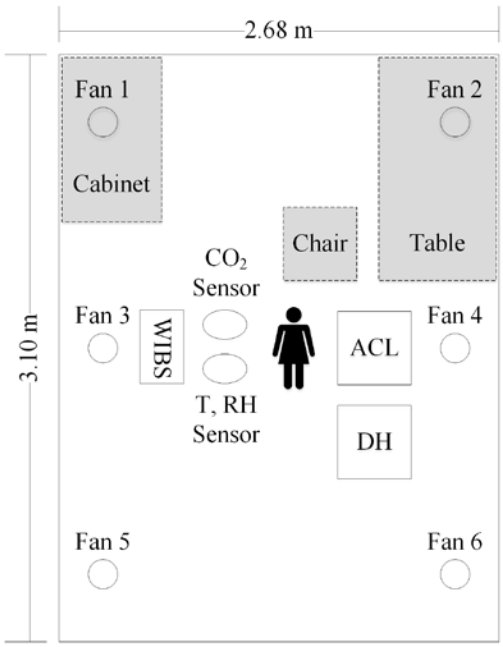

Figure 1. Configuration of the experimental room, including the location of furniture and instruments. (ACL: air cleaner, DH: dehumidifier)

The room is served by a central air-conditioning and mechanical ventilation (ACMV) system and has its own ACMV supply duct. To isolate the effect of indoor emissions and to slow the rate of bioaerosol removal (so as to facilitate accurate measurement), we took these three actions: i) shut off the air supply to the room during the experiments, ii) covered the ceiling and the door louver with antistatic plastic film (CFB9600 series, Anti-static cleanroom films, CFB, Inc., Orange, CA, USA), and iii) sealed the cracks around the door with sealing strips (10 m × 9 mm × 5.5 mm EPDM rubber brown sealing strip, Stormguard, Inc., Macclesfield, Cheshire, UK). Consequently, air-exchange to the room was limited to infiltration. The air-exchange rate (AER) was determined to be 0.06 ± 0.01 per hour (Table S1, n=36), as determined by means of carbon dioxide (CO_2) tracer decay tests. Six mini USB powered fans (blade diameter = 88 mm, two blades) were used to maintain a well-mixed condition without excessive airflow.

Three Asian female volunteers, referred as to F1-F3, participated as subjects in the experiments. They were all at the age of about 30 years, and with shoulder length hair, but differing in height and weight (F1 – 1.72 m, 59 kg; F2 – 1.50 m, 40 kg; F3 – 1.61 m, 49 kg). The influence of gender and race on emission rates is outside the research scope of this study. Metabolic carbon dioxide emission rates during each bioaerosol emission test were determined by means of material balance, with the occupant being considered as the sole source for CO_2 above the baseline value. In these experiments, the mean metabolic carbon dioxide emission rates for participants F1, F2, and F3 were 49, 40, and 45 g per h, respectively. The activity intensity was estimated to be in the range 1.8-3.2 mets (1 met = 1 metabolic equivalent of task = 58.2 W per m^2 of skin surface area) when they were executing the scripted walking task (Jetté et al., 1990).

The primary experiments were designed to explore the potential influence of two factors — relative humidity and application of skin moisturizer — expected to alter skin conditions and therefore influence bioaerosol emissions. We tested two relative humidity conditions and two skin moisturizer states using a 2 × 2 experimental matrix. Recognizing that these experiments are conducted in a tropical environment in which the absolute ambient humidity is consistently high, the two RH levels tested were 60-70% (denoted 'H') and 40-45% (denoted 'L'). The two skin moisturizer states were with application over the torso, arms and legs (denoted 'M') and without application (denoted '0'). Thus, for each participant, the tested conditions were as follows: '**H0**', the RH of room air was 60-70% and the subject did not apply the moisturizer before experiments; '**L0**', the RH of room air was 40-45% and the subject did not apply the moisturizer; '**HM**', the RH of room air was 60-70% and the subject applied the moisturizer; and '**LM**', the RH of room air was 40-45% and the subject applied the moisturizer. For each of the four

conditions and each of the three subjects, experiments were conducted with three replicates. Table S1 in the supporting information provides full details about the schedule and conditions for each experimental run. We scheduled up to two experiments for each study day, usually with one subject involved in a morning test and another subject involved in an afternoon test. There were some occasions in which the same subject was used in both tests in a single day owing to the availability of subjects and the experimental room. In these cases, we allowed ~ 6-h rest period between the two tests.

Pure jojoba oil was selected as the moisturizer because it closely resembles sebum, a waxy substance produced by human skin glands (Wisniak, 1987). In addition, jojoba oil itself without agitation by human activity was not expected to be an indoor source for particles, as confirmed by the supplementary experiments (R43-R44 in Table S2). The possibility of microbial growth during each experimental test is limited because the pure jojoba oil is not a favorable medium (Guirguis et al., 2013). In addition, the duration of each test (~ 80 min including acclimation period) does not allow for much microbial reproduction (Meletiadis et al., 2001; Wang et al., 2015).

We regulated the amount of moisturizer (D_n, ml) using equation 1. The dose of moisturizer per unit body surface was set to be uniform for each of the three subjects (uD, 4 ml per m^2 body surface). The body surface area (S, m^2) for each subject n was estimated based on height (H, m) and weight (W, kg) (Mosteller, 1987). The amounts of moisturizer applied were similar for the three subjects (approximately 7 ml for F1, 5 ml for F2, 6 ml for F3).

$$D_n = uD \times S_n = uD \times \sqrt{\frac{H_n \times W_n}{36}} \quad (1)$$

Each experimental run comprised two consecutive test periods: (i) a human emission test period (denoted ‘E’); and (ii) a baseline test period (denoted ‘B’). Prior to each E test, we carried out a few pretreatment steps to prepare the room and the participant for the experiment. The pretreatment of the experimental room included these steps: i) flushing the room with the cooled air in the hallway to remove residual CO_2 and excessive heat; ii) vacuuming the floor to diminish the influence of particles resuspended from vinyl flooring; iii) operating a portable air cleaner, and, if required, a portable dehumidifier, for about 50 min to reduce the initial indoor concentrations and to manipulate the RH to its target value. Only one participant was involved in each E test. The preparation of the participant entailed these steps: i) showering using plain and gentle shower gel (fragrance free body wash, JĀSÖN); ii) applying moisturizer over the torso, arms and legs, if required, before changing to the freshly laundered sleeveless shirt and trousers that the researchers had prepared (all were made of 100% cotton and in black colour); iii) being seated in the acclimation room for about 30 min and then moving to the experimental room; and iv) being seated in the experimental room for another 20 min. During the active experimental period, the subject walked in place in the experimental room, in time with a metronome set at a rate of 100 beats per minute. The walking-in-place motion was maintained for 30 min, beginning right after the air cleaner and dehumidifier, if used, were stopped. It is worth noting that we operated the air cleaner and dehumidifier in the experimental room during steps iii) and iv).

Each participant wore her own shoes when walking, but she was required to brush the sole and upper surface of the shoes, and to put on overshoes (non-woven spun bond polypropylene upper and a Latex/PE sole, Pal International Ltd., Lutterworth, Leicestershire, UK) before entering the experimental room. We also requested the participants to tighten hair into a bun and to minimize coughing and speaking activities during experiments. All the subjects were in good

health throughout the experiments. After each experimental (E) test, a background (B) test was conducted. The procedure for the B test was the same as in E, except that there was no subject in the room.

The acclimation room is an office situated next to the experimental room with ventilation and thermal control provided from a central ACMV system. The particulate matter concentration, air temperature and RH in this room were adjusted to the desired acclimation conditions ($PM_{2.5}$ <0.1 $\mu g/m^3$ and T = 26±1 ^oC for all cases, RH = 42±2% for low RH conditions, RH = 65±3% for high RH cases). Overall subject acclimation was conducted in two rooms (30 min in the acclimation room plus 20 min in the experimental room) rather than all 50 min solely in the experimental room. The reason for split acclimation was to reduce CO_2 accumulation and associated subject exposure in the experimental room. The CO_2 concentrations throughout each of the 36 emission tests (E) did not exceed 1500 ppm in the experimental room. The selection of a 50-min period for acclimation is based on previous work by Cravello and Ferri (2008), which found that changes in skin hydration levels owing to different climate conditions occurred in an adaptation period of about 30 min. The study procedures were approved by the Institutional Review Board at the Nanyang Technological University (IRB-2015-07-011).

Indoor air in the experimental room was sampled from a location near the center, at a height of 1.1 m, which approximates the breathing height of a seated occupant. Hallway air was sampled at the same height, at a location approximately three meters from the door leading to the experimental room. A Waveband Integrated Bioaerosol Sensor (model WIBS-4A, Droplet Measurement Technology, Inc., Boulder, CO, USA) was placed inside the experimental room, measuring the size, asymmetry factor, and fluorescence characteristics of each sampled particle

with millisecond time resolution. The next section provides more detailed information about the use of the WIBS in this study.

Several monitors were used to collect additional environmental data, including temperature and relative humidity (T, RH; VelociCalc Model 9545-A, TSI, Inc., Shoreview, MN, USA), carbon dioxide level (CO_2; Model CM-0018, CO_2 meter, Inc., Ormond Beach, FL, USA), and particle concentration (Optical Particle Sizer, Model 3330, TSI, Inc., Shoreview, MN, USA). Each instrument logged data at 3-min sampling intervals, consistent with how the WIBS data were interpreted. The environmental data obtained both in the experimental room and in the hallway were relatively stable across the 36 primary experiments (except CO_2 and $PM_{2.5}$ concentrations in the experimental room owing to the strength of emissions from the human subject). The T, RH, CO_2 and $PM_{2.5}$ concentrations in the hallway were 27±0.5 °C, 53±2%, 670±50 ppm, and 0.5±0.2 μg/m^3, respectively. The environmental data in the experimental room for each of emissions and baseline tests is summarized in Table S1.

2.2 WIBS instrument

The version of the WIBS (model WIBS-4A) that we used in this work has a total flowrate of 2.5 L/min (2.2 L/min for sheath flow and 0.3 L/min for aerosol sampling). The measurement principles are described in the instrument manual (DMT, 2013) and also reported in previous studies (Crawford et al., 2015; Perring et al., 2015). Briefly, the elastically scattered light intensity, resulting from the interception of a continuous-wave 635 nm diode laser beam, was used for particle sizing. We used the factory calibration of the WIBS, which is based on light scattering by spherical particles of polystyrene latex (refractive index = 1.58), to convert scattered light intensity to optical particle size. In addition, the forward scattered laser light is imaged onto a quadrant photo detector. The asymmetry factor (AF) for each particle is estimated

from the variability of scattered light in relation to viewing angle. The AF may be interpreted as an indicator of the shape of particles. The AF scale varies between zero and 100; particles that are more nearly spherical have smaller AF values while elongated particles would tend to have higher AF values. Two pulsed xenon UV sources (280 nm and 370 nm, also referred to as Xe1 and Xe2) and two fluorescence detection channels (310-400 nm and 420-650 nm, also referred to as FL1 and FL2) provide three types of fluorescence signals. The following labels are used in this work: Channel A refers to a signal detected by the FL1 detector following Xe1 excitation, Channel B refers to a signal detected by the FL2 detector following Xe1 excitation, and Channel C refers to signal detected by the FL2 detector following Xe2 excitation. The Xe2/FL1 measurement is ignored as the FL1 detector becomes saturated with elastically scattered UV light.

Not all particles passing through the cavity of WIBS will be irradiated because of the maximum flash rate (125 Hz) of the xenon lamps. In this study, the number of particles that were missed by the flash lamp accounts for less than 5% of total particles that pass through the laser beam. A particle detection threshold for a full particle measurement was set at a value of 8 in this work, which corresponds to a minimum detectable particle diameter of ~ 0.5 μm. A force-trigger measurement using WIBS was carried out for at least 15 minutes after each B test. In the force-trigger mode, the flash lamps are triggered automatically (at a frequency of around 2 Hz) without particles in the cavity. The fluorescent thresholds found in the force-trigger mode allow determination of which particles are considered to be fluorescent and within which channel(s) of detection. In this study, particles were classified as fluorescent if they produced signals at least 3 standard deviations above the mean of the forced trigger intensity for a given channel. Following annotation introduced by Perring et al. (2015), we classified particle fluorescence into eight types

according to whether the fluorescence signal was above the fluorescence threshold or not in each of the three channels. As indicated in Table S3 in the Supporting Information, we labelled particles that did not exhibit fluorescence above the threshold in any channel as type "non"; particles that exhibited fluorescence above the threshold in only one channel were labeled as type "A," "B," and "C," respectively; particles that exhibited fluorescence above the threshold in only two channels were labelled as type "AB," "AC," and "BC," respectively; and particles that exhibited fluorescence above the threshold in all three channels were designated as type "ABC."

2.3 Data interpretation

The WIBS data were analyzed via a user-written program based on the R platform. The occurrence and characteristics of each airborne particle with millisecond resolution were processed to assess time-resolved, size-resolved, and fluorescence categorized number concentrations. Particles concentrations were assessed with 3-min time resolution utilizing 14 size channels (0.47-0.58, 0.58-0.72, 0.72-0.90, 0.90-1.12, 1.12-1.39, 1.39-1.73, 1.73-2.16, 2.16-2.69, 2.69-3.34, 3.34-4.16, 4.16-5.18, 5.18-6.45, 6.45-8.03, and 8.03-10 μm). Channel sizes were set to maintain a constant logarithmic spacing ($dlog_{10}(d_p) = 0.095$). In assessing the size distribution of emission rates, we focus on particles in largest 11 size channels in the diameter range 1.0-10.0 μm, as the WIBS possesses limited counting efficiency for submicron particles (Healy et al., 2012b; Perring et al., 2015). When reporting mean emission rates, we aggregated the results into three integrated size ranges (1.0-2.5, 2.5-5.0, 5.0-10.0 μm), recognizing the conventional and regulatory sorting of aerosol particles.

Occupant emission rates of particles ($ER_{k,i,j}$, in units of particles per person-h) were evaluated using a time-integrated material-balance model (equation 2). The first term in equation 2 is the emission rate determined from the test having one subject walking in the room

(test E), while the second term is the background rate estimated for the vacant room (test B). In the equation, ΔC is the concentration difference between the start and end of the test (in units of particles/m^3); $\bar{C}$ is the mean concentration measured throughout the test period (particles/m^3); and V is the experimental room volume (m^3). The subscripts k, i and j denote particle fluorescence type, particle size group, and the index number of the experiment, respectively. Finally, AER is the air exchange rate (per h), β is the first-order particle deposition loss rate coefficient (per h), and t_E and t_B are the duration of the experimental and background periods (h), respectively.

$$ER_{k,i,j} = \frac{V \times \left[\Delta C^{E}_{k,i,j} + \overline{C^{E}_{k,i,j}} \times (AER + \beta) \times t_E\right]}{t_E} - \frac{V \times \left[\Delta C^{B}_{k,i,j} + \overline{C^{B}_{k,i,j}} \times (AER + \beta) \times t_B\right]}{t_B} \quad (2)$$

2.4 Supplementary experiments

Supplementary experiments (R37-R42 in Table S2) were undertaken to determine the deposition loss coefficients (β) used for data analysis in this work. As indicated in Figure S1 in Supporting Information, the size-specific coefficients (mean ± standard error) obtained in supplementary experiments were substantially lower than the values reported by Thatcher et al. (2002), especially for the larger particles. The reduction is probably a consequence of different size measurement techniques (optical diameter used in this work whereas aerodynamic diameter was employed in the study by Thatcher et al.) and also intrinsic particle properties (e.g. shape, density, etc.). We also conducted supplementary experiments to confirm that the jojoba oil itself (evenly applied to plastic film and without motion) would not be an indoor emission source without human occupancy (R43-R44) and to test whether clothing color (R45-R47) and detergent use (R48) was important in this work. We did not observe a discernible influence of

either of these two factors. The conditions for each supplementary experimental run and detailed discussion are presented in Table S2 and Appendix S1, respectively.

2.5 Quality control

The WIBS was calibrated in the laboratory of Droplet Measurement Technology (DMT) before being transported to Singapore. The calibration used a range of monodispersed polystyrene latex (PSL) particles in the diameter range 0.8-4.0 μm. In Singapore, we checked the calibration using 1.005 μm and 2.005 μm PSL particles (JSR Life Science Inc., Minato-ku, Tokyo, Japan). The differences between WIBS responses of particle size and the physical diameters of selected PSL particles was less than 10%.

We conducted side-by-side (SBS) tests of the OPS and CO_2 meters in a carpeted and occupied office for 4 hours with indoor $PM_{2.5}$ and carbon dioxide concentrations in the ranges 20-30 $\mu g/m^3$ and 600-1200 ppm, respectively. As reported by Zhou et al. (2015), the purpose of the SBS tests is to reduce the relative bias in concentrations measured by different instruments. The OPS and CO_2 meter used in hallway in the primary experiments were recently calibrated and were selected as reference instruments. The adjustment factors summarized in Table S4 were applied to correct biases.

3. Results and Discussion

3.1 Mean emission rates

Figure 2 presents a summary of mean emission rates decomposed by particle size (left panels) and fluorescence type (right panels) for total aerosol particles in the case of high RH conditions (60-70%) for each of the three subjects. Analogous plots for each of three participants for each of four experimental conditions showing decomposition by particle size and fluorescence type are presented in the Supporting Information: Figures S3 for total aerosol

particles (ER_T) in the case of low RH conditions (40-45%) and Figures S4-S5 for fluorescent particles only (ER_F) in both RH conditions.

For the cases with high RH and no moisturizer ('H0', top panels in Figure 2), the mean emission rate of total fluorescent aerosol particles (ER_F) varied little across the three participants: 6.8-7.5 million particles per person-h. The fluorescent particles constituted about half of the total count-weighted emissions (ER_T). Three fluorescence categories of particles (ABC, A, and AB) combined to account for more than 90% of ER_F. Particle size decomposition indicates that, by number, particles in the diameter ranges 1.0-2.5 and 2.5-5.0 μm dominated, with these aggregated two sections combining to contribute more than 80% of the total emission rate. The dominance of these sizes by count was true both for total and for fluorescent aerosol particles.

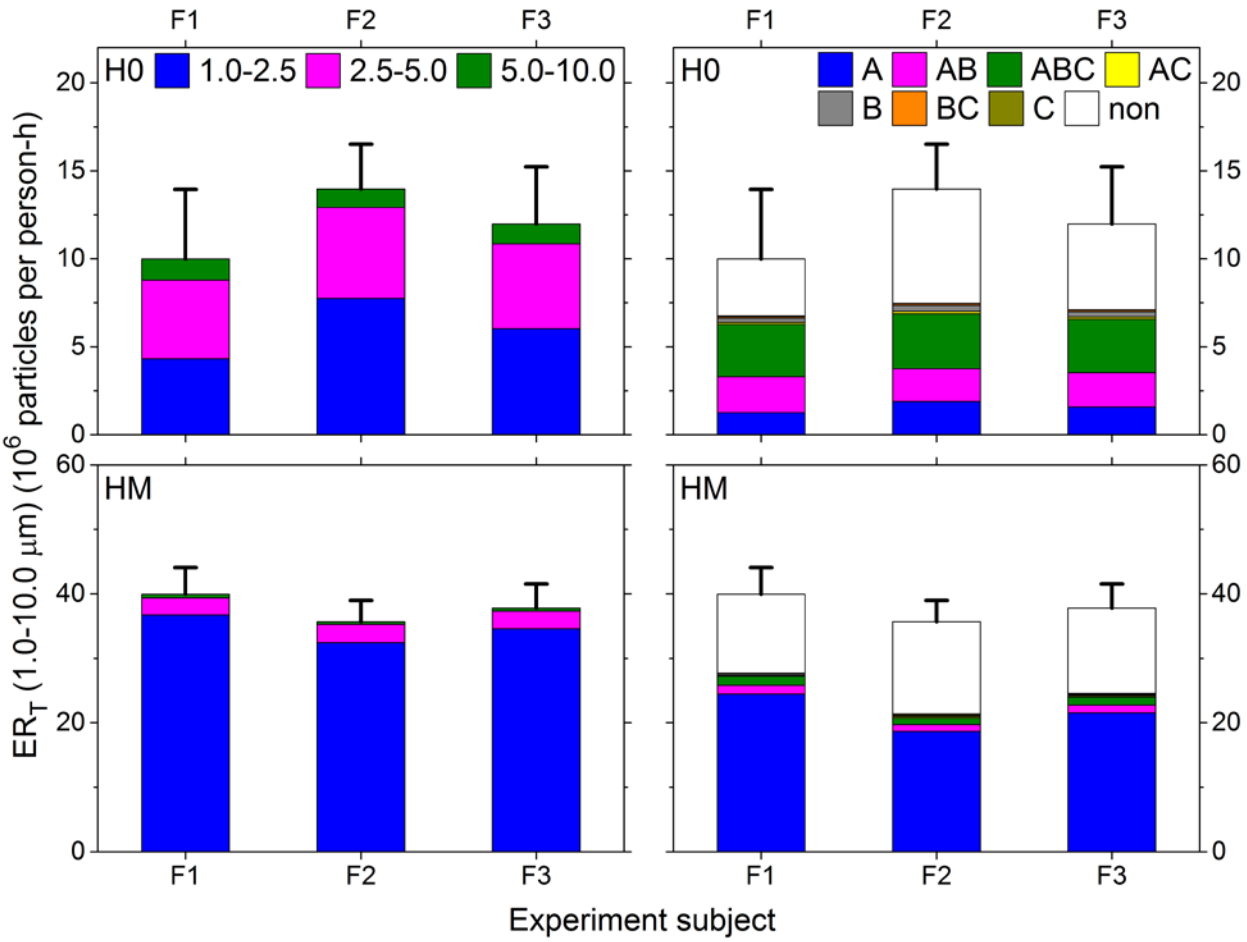

Figure 2. Average count-weighted emission rates of total aerosol particles for the three subjects (F1-F3), decomposed by particle size (left) and by fluorescence category (right). All cases are for high RH conditions (60-70%). The upper panels are for cases without moisturizer (H0) and the bottom panels are for cases with skin moisturizer applied (HM). Note that different vertical scales are used on the upper and lower frames. The whiskers represent variability of total emission rates as ± standard errors.

Surprisingly, the use of moisturizer was associated with an increase in the number-weighted emission rates by a factor in the range 2-5 for both total and fluorescent aerosol particles. The substantial increment was attributable to enhanced emissions of fine particles (1.0-2.5 μm). Mainly, these particles were categorized as either type A or nonfluorescent.

We found that the mean fluorescent particle number emission rates measured at low RH conditions were comparable to or slightly lower than the values obtained in high RH conditions.

In their work, Bhangar et al. (2016) found that walking on carpet at a low relative humidity (<40%) was associated with substantially lower (by a factor of 2.5) emissions than occurred in higher humidity (80%). We note that the particles emitted in this work were mainly associated with shedding from the human body envelope (including clothing), whereas the research of Bhangar et al. would have included resuspension from carpeting. We had anticipated that the lower humidity conditions would be associated with higher emissions owing to increased friction between skin and fabric fibers along with more easily detachable squames at lower humidity. We find surprising the tendency of emission rates of fluorescent particles to be higher under the higher humidity condition. The reason for the unexpected observation is unknown. Pan et al. (2014) found high RH (50-80%), with presence of ozone (150 ppb), could increase the 351/355-nm-excited fluorescence (emission at 430-580/380-700 nm). However, this finding cannot be generalized to the present work because of different experimental conditions. Another hypothesis is an increase in skin friction under humid conditions. As reviewed by Hendriks and Franklin (2010) and Veijgen et al. (2013), higher hydration levels of stratum corneum under humid conditions would lead to higher coefficients of friction between skin and contact materials.

The count-based emission rates are used to estimate mass-weighted emission rates, based on the assumptions that particles had a density of 1 g/cm^3. It is acknowledged that the mass-weighted emission rates are subject to high uncertainty because information about particle size- and type-resolved density is limited. However, these estimates provide insight about the importance of coarse particle emissions with regard to particle mass, which may be valuable for health risk evaluation and would be overlooked when only interpreted with count-based data. Results are summarized for the total and fluorescent particles for all four experimental conditions in Figures S6-S7 and Figures S8-S9, respectively. For cases without the use of moisturizer, the

mean emission rates of total aerosol particles for the three subjects averaged about 0.33 mg per h and about 90% of the mass was associated with fluorescent particles. The dominant contribution (more than 60% of the total) was from coarse-mode ABC-type particles. For cases with use of moisturizer, although the count-weighted emission rates were higher, mass-weighted particle emissions *decreased* by about one-third both for total and for fluorescent particles. This decrease was mainly attributable to the reduction of coarse particle emissions with the moisturizer application, which outweighed the enhanced fine particle emissions.

As displayed in Figure S10, although the mean emission rates were similar across the three subjects, replicate experimental runs displayed high variability in some cases. Sources of variability could include variations in the contributions from baseline experiments, differences in clothing, incomplete acclimation, and variability in instrument response. Appendix S2 in the supporting information presents a discussion about variability. Overall, the differences in mean emission rates among participants were small compared with the variability among replicates.

Considering the seven categories of fluorescent particles, three types exhibited appreciable emissions: categories ABC, A and AB. In following sections, we focus on these fluorescence categories as we further describe the influence of RH and moisturizer on the size distribution of emissions and particle shape.

3.2 Size distribution of emissions

Figures 3-5 present size distributions of weighted mean (± standard error) emissions of ABC, A, and AB particles, respectively, for participant, F1. Analogous plots for the other two participants for these primary particle fluorescence categories are presented in the Supporting Information (Figures S15-S20). The four frames in each figure correspond to the four cases investigated in this work. The influence of the two independent variables can be explored by

comparing the frames in the same row (moisturizer) and the same column (humidity), respectively. Note that the emissions are plotted on the same scale (0-20 million particles per person-h), except that a larger scale (0-100 million particles per person-h) is applied to category A particles because of enhanced emissions with the use of moisturizer. Lognormal distributions with an offset (equation 3) were fitted to mean emissions in the 1-5 μm diameter range (except that a narrower diameter range, 1.5-5 μm, was applied for category AB particles in the cases with moisturizer). Each panel displays a summary of best-fit parameters — geometric mean diameter (d_g, μm), geometric standard deviation (ln σ_g, -), offset (y_0, $\times 10^6$ particles per person-h), area above the offset (A, 10^6 particles per person-h × μm) of the lognormal peak, and adjusted coefficient of determination (adj. R^2, -). Curve fitting was done via the software OriginPro (version 2015).

$$y = y_0 + \frac{A}{x\sqrt{2\pi}\ln(\sigma_g)} e^{\frac{-[\ln\frac{x}{d_g}]^2}{2(\ln\sigma_g)^2}} \quad (3)$$

The use of moisturizer suppressed the emission of fluorescence type ABC particles. As illustrated in Figure 3, for subject F1, the use of moisturizer was associated with a ~50% reduction in emission peak amplitude (the maximum height of size distribution from the offset), for both high and low RH conditions. The geometric mean size for type ABC particles did not exhibit a clear shift with moisturizer use or with humidity: the diameters were approximately 4 μm across the four conditions, for all three subjects.

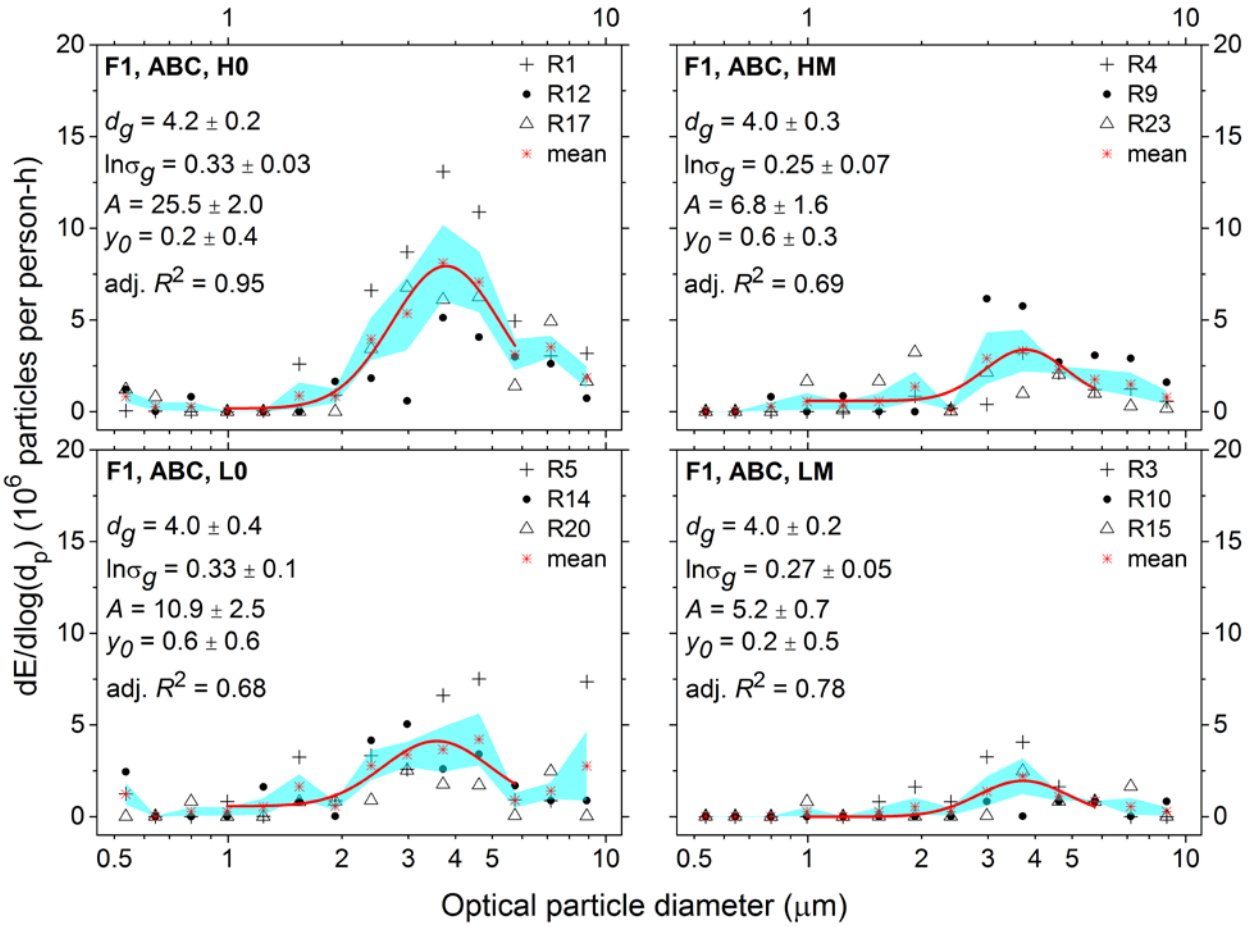

Figure 3. Size distributions of count-weighted mean (± standard error) emissions of ABC particles for subject F1. Experimental conditions are noted at the top left of each panel: (H0) high RH without moisturizer; (HM) high RH with moisturizer; (L0) low RH without moisturizer; and (LM) low RH with moisturizer. Emissions are shown as a function of optical particle diameter. The geometric mean diameter (d_g, μm), geometric standard deviation (ln σ_g, -), offset (y_0, ×10^6 particles per person-h), area above the offset (A, 10^6 particles per person-h × μm), and adjusted coefficient of determination (adj. R^2, -) of the lognormal peak that provide the best fit to mean emissions in the 1-5 μm diameter range are shown in each panel. The shaded areas represent variability of results as ±standard error. The ID for each experimental test is noted on the top right corner of each frame.

The use of moisturizer produced a different result for category A particles as compared to ABC particles (Figure 4). The use of moisturizer was associated with much higher emission rates for A particles than was observed when moisturizer was not applied. The A particles exhibited a peak at a smaller diameter (1.5-2 μm) than was observed for the ABC category particles.

Moisturizer was also observed to affect the size distribution of emitted nonfluorescent particles. As indicated in Figure S21, the size distribution of nonfluorescent particles generally followed the pattern we observed in plots of A particles, with an emission peak in the fine mode.

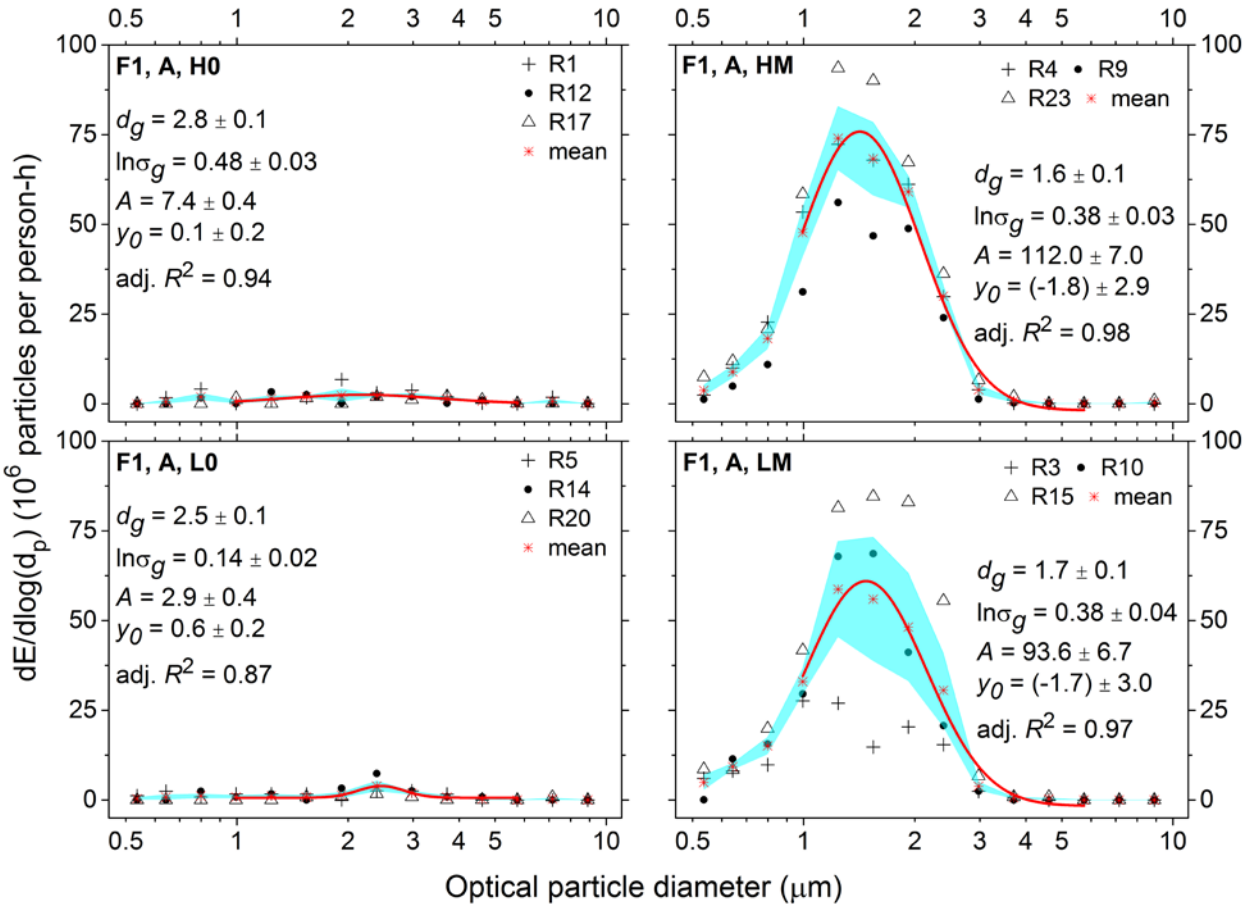

Figure 4. Size distributions of count-weighted mean (± standard error) emissions of A particles for subject F1. Please refer to Figure 3 for detailed notation.

Among the three fluorescent categories, the AB particles exhibited the weakest dependence on experimental conditions. The range of emission peak amplitudes for subject F1 spanned only a factor of ~1.5 (from ~5 to ~7.5 million particles per person-h). As displayed in Figure 5, only the case of high humidity without moisturizer always exhibited a prominent lognormal peak with a geometric mean size at around 2.5-3 μm.

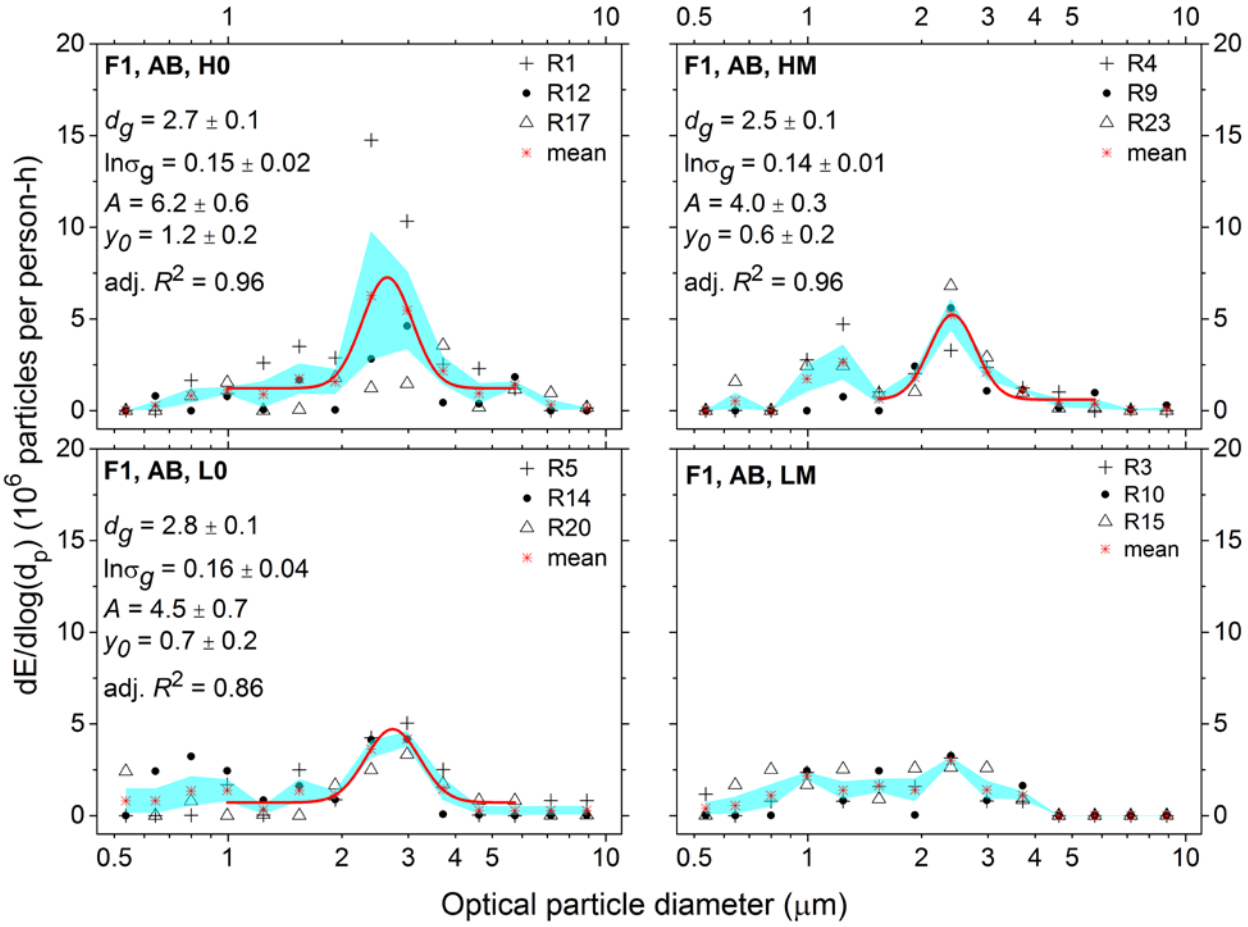

Figure 5. Size distributions of count-weighted mean (± standard error) emissions of AB particles for subject F1. Please refer to Figure 3 for detailed notation. In the case with moisturizer at high RH (HM), mean emissions in the 1.5-5 μm diameter range are used in the fitting. In the case with moisturizer at low RH (LM), the fitting is not included in the presentation because of adj. R^2 < 0.5.

For all three primary fluorescence categories of emitted particles, we did not see a discernible influence of RH on the geometric mean diameter. In most cases, the lower air humidity was associated with a reduction in emission peak amplitude of the different fluorescent particle categories, a result that is consistent with the findings revealed in §3.1 — a slightly lower emission rate measured at low RH conditions. For subject F1, the ratio of low-humidity to high-humidity peak amplitudes for the five cases (with or without moisturizer for fluorescence

categories ABC and A, and without moisturizer for category AB) exhibited an average ± standard deviation of 0.84 ± 0.46.

3.3 Size-integrated asymmetry factors

Across all the experiment tests, we observed a tendency for the asymmetry factor (AF) to increase with increasing particle size, indicating more aspherical shape for larger particles. This feature is illustrated in Figure 6, in which the particle size is clustered into three groups, the three main fluorescence categories are presented, and two separate experimental runs are considered, one without moisturizer (H0, left) and one with moisturizer (HM, right). The two experiments were conducted with the same subject (F1) and same air humidity level (60-70%).

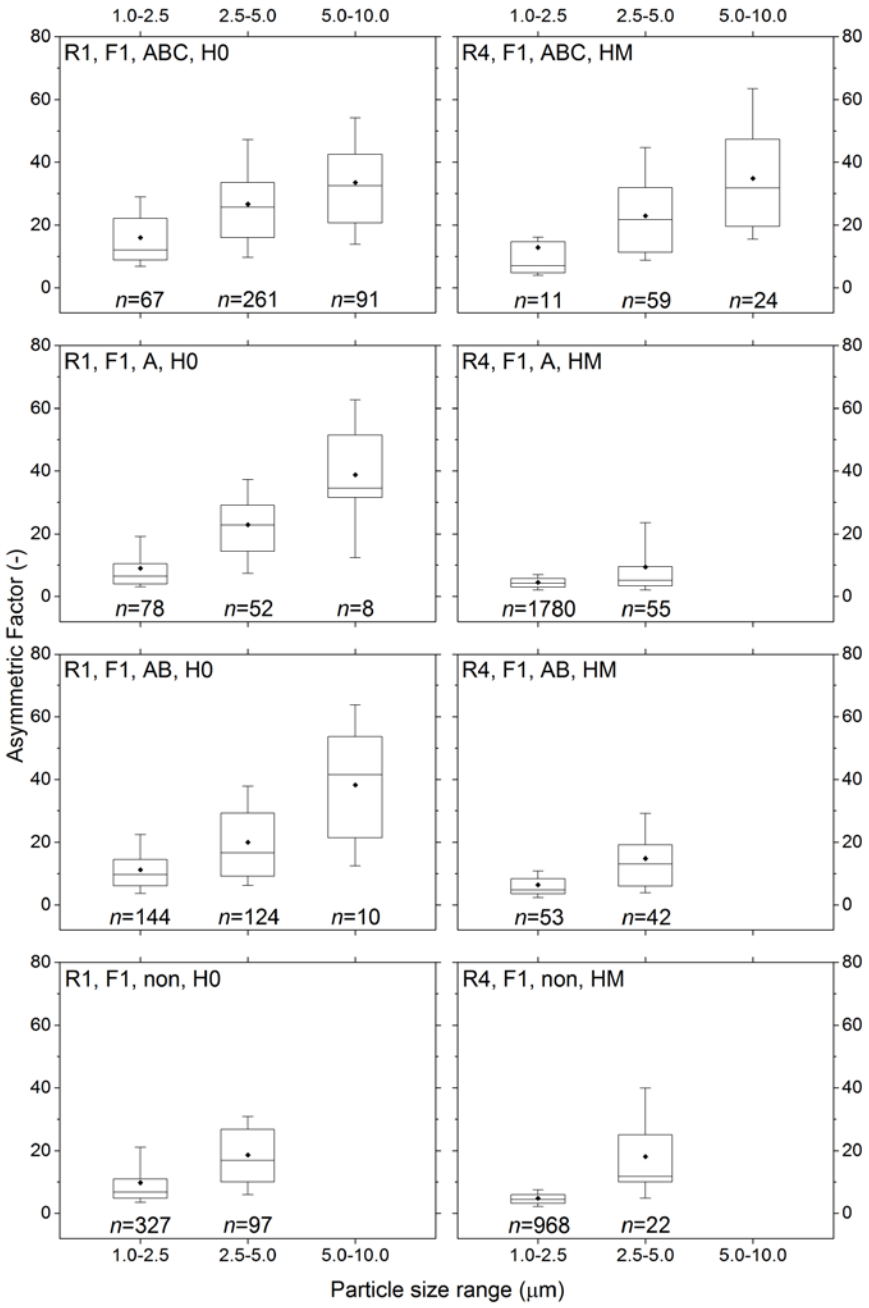

Figure 6. A comparison of asymmetry factors evaluated under experimental conditions H0 (left) and HM (right) for subject F1. The ABC, A, AB, and nonfluorescent particles were categorized into three aggregated size clusters (diameters 1.0-2.5, 2.5-5.0, and 5.0-10.0 μm). Solid circle is the mean; whiskers correspond to the 10th and 90th percentiles; upper and lower bounds of the box represent 25th and 75th percentiles; solid line within box is the median. The symbol *n* indicates the number of particles in ~ 9 L of chamber air as analyzed by the WIBS instrument in the 30-min experiment. In the case with moisturizer (R4), too few particles ($n < 5$) were observed in the 5-10 μm range to include categories A, AB, and nonfluorescent in the presentation.

Without moisturizer, all three types of fluorescent particles exhibited higher AFs as particle size increases. Specifically, the mean AFs are ~10, ~20, and >30 for particles of diameter in size range 1.0-2.5, 2.5-5.0, and 5.0-10 µm, respectively. The AF distributions measured in experiments with moisturizer use followed the increasing trend with particle size, except for the relative stable values (mean AFs = 4-6) for category A particles. However, too few particles were observed in the 5-10 µm range to include categories A and AB in the presentation. We emphasize that the observation of higher AFs for larger particles was not unique to fluorescent particles; it was also displayed for nonfluorescent particles.

3.4 Comparing results with Bhangar et al. (2016)

The study most closely related to the one reported here is by Bhangar et al. (2016), which characterized emissions of fluorescent biological aerosol particles as a consequence of occupant activities in a chamber. That work utilized the ultraviolet aerodynamic particle sizer (UV-APS). Other primary differences from the present effort included conducting the study in a temperate (rather than tropical) climate, considering a broader range of occupant activities, operating with higher background particle levels, and utilizing a carpeted chamber.

Without moisturizer, the mean emission rate of total particles larger than 5 µm in our study was in the range 0.4-1.2 million particles per person-h, lower than the value of 3 ± 1 million particles per person h reported by Bhangar et al. (2016). Among the factors that may have influenced emissions differences were that our subjects systematically showered before each experiment; changed into freshly laundered clothing; and we consistently applied measures to minimize resuspension from the floor and shoes. In addition, differences in body coverage and texture of clothing, walking pace, subject demography between two studies, may also have contributed to the different results.

For conditions of walking on a floor covered by plastic (with RH < 40%), Bhangar et al. (2016) reported mean emission rates of size-integrated (2.5-10.0 μm) fluorescent particles to be 1.7±0.5 million particles per person-h. This value agrees with our result — 1.4-1.6 million particles per person-h — for category ABC particles emitted under comparable experimental conditions: case L0, with low RH and without moisturizer. In a side-by-side comparison measuring FBAP in the atmosphere, Healy et al. (2014) have demonstrated that the responses from WIBS channel C (mainly ABC particles in this work) are strongly correlated with UV-APS results.

The size distributions of emitted fluorescent particles conform well to lognormal distributions both in this work and as reported by Bhangar et al. (2016). The ABC particles emitted in this work exhibit a lognormal peak with a geometric mean diameter of ~ 4 μm. The value is within the range of 3-5 μm, which Bhangar et al. reported as the mode of fluorescent particles.

3.5 On measuring particle fluorescence to detect bioaerosols

Measurements based on particle fluorescence offer the possibility of studying dynamic processes in indoor environments that operate on short time scales and that vary with particle size. Currently available culture-based and DNA-based analysis methods do not have that potential. Nevertheless, the validity of using fluorescent particle observations as a proxy for bioaerosols is a topic of debate. In addition to the fluorescence methods lacking biological specificity, there are potential fluorescent artifacts arising from abiotic materials. Furthermore, some bioaerosols show weak or no fluorescence.

Among the three categories of fluorescent particles associated with human activity, one should not rule out that any one of them might be fluorescent biological aerosol particles

(FBAPs). A mixture of bacteria, fungi and pollen can display the fluorescence types of ABC, AB, and A, based on previous fluorescence spectra characterization studies (Wlodarski et al., 2006; Healy et al., 2012; Hernandez et al., 2016), which that found common airborne biological particles present diverse fluorescence patterns. Fungi and pollen, which are commonly abundant in outdoor air, may be evident in occupant-associated emissions because of the release of the particles previously deposited on clothing, e.g. during laundering.

The enhanced emissions of category A particles owing to the use of moisturizer might be a consequence of an abiotic process, considering that previous work has demonstrated abundant abiotic interferences in fluorescence channel A (Pöhlker et al., 2012). Human activity would be a prerequisite to aerosolize applied jojoba oil and therefore result in enhanced emissions, a feature indicated by the supplementary experiments, which demonstrated that an exposed, stationary film of jojoba oil is not an indoor source of particles.

Asymmetry factor (AF) data have been used in hierarchical agglomerative cluster analysis (Gabey et al., 2013; Crawford et al., 2015) and in a fluorescence spectra characterization study (Healy et al., 2012b) to probe airborne particle types. However, using AF data for discrimination of biological particles in this work would require deeper investigation, beyond the scope of the present effort. The tendency for AF to increase with increasing particle size was observed for both fluorescent and nonfluorescent particles. A calibration method for AF detection is not well established. Further studies that couple microscopic methods with time-resolved sampling are warranted to improve insight into the AF data and their interpretation as an indicator of particle shape in bioaerosol studies.

4. Conclusions

This study is the first to apply the WIBS to evaluate human emission rates of fluorescent biological aerosol particles (FBAP). We characterized FBAP emissions from the human body envelope when walking indoors. The research design minimized contributions from particle resuspension through the use of a room with vinyl flooring that was cleaned before each test. We used dark-coloured clothing to minimize any confounding associated with fluorescent brightening agents and the clothing was freshly laundered to minimize uncontrolled emissions associated with prior loading of biological particles onto the fabric through wearing and/or environmental exposure.

Across three female subjects, the mean emission rates of total supermicron fluorescent particles associated with human walking were in the range 6.8-7.5 million particles per person-h (~0.3 mg per person-h) for baseline conditions in which the chamber RH was 60-70% and the participant did not apply moisturizer after showering. The fluorescence of the particles was mainly associated with types ABC, AB, and A, which together accounted for more than 90% of total fluorescent emissions. Among the three fluorescence categories, ABC particles were particularly important, contributing more than 40% and 70% to total number and mass emission rates of fluorescent particles, respectively. Lognormal size distributions describe reasonably well the three categories of fluorescent particles emitted, with ABC particles exhibiting a lognormal peak with a geometric mean diameter at approximately 4 μm, somewhat higher than the approximately 2.5 μm seen for AB and A particles. The asymmetry factors of all three categories of fluorescent particles, and also for nonfluorescent particles, followed increasing trends with particle size.

Surprisingly, the use of moisturizer was associated with a significant increase in the number-weighted emission rates (by factors in the range 2-5), but, because the moisturizer-associated emissions were shifted to smaller particle sizes, the mass emission rate was lower with moisturizer than without. Looking more closely, we observed that the use of moisturizer was associated with enhanced emissions of fine particles manifesting as fluorescence type A and decreased emissions of coarse particles. The enhanced emissions of A-type particles with moisturizer use may have been an indication of an abiotic interference. These particles exhibited a prominent peak with a geometric mean diameter at approximately 1.5 μm and were more spherical (with mean AFs at ~ 4-6) than the coarse-mode fluorescent particles emitted without moisturizer. The mean emission rates did not vary significantly between the case of low and high RH conditions, but the lower air humidity was associated with a reduction in emission peak amplitudes of the different fluorescent particle categories.

The experimental procedure undertaken here could fruitfully be applied to explore additional aspects of this system: i) other factors that are expected to alter the frictional interaction between human skin and clothing (e.g., different clothing fabrics) and ii) the suspension of particles that were previously loaded onto clothing (e.g., from clothing exposed to the environment and/or worn substantially before testing). Although previous studies have demonstrated that pure cultures of bacteria, fungi and pollen recovered from both indoor and outdoor environments display a broad range of fluorescence patterns, including the three types (ABC, AB, and A) observed in this work, it is not yet conclusive that the fluorescent particles measured in this work represent occupant-associated bioaerosols. Future collaborative work with DNA-based methods could usefully evaluate to what extent the UV-LIF technique captures the biological components in the air of built environments.

Acknowledgements

Financial support for this research was provided by the Republic of Singapore's National Research Foundation through grant NRF-CRP8-2011-03 and through a grant to the Berkeley Education Alliance for Research in Singapore (BEARS) for the Singapore-Berkeley Building Efficiency and Sustainability in the Tropics (SinBerBEST) Program. BEARS has been established by the University of California, Berkeley as a center for intellectual excellence in research and education in Singapore.

Supporting Information

Additional supporting information includes the following materials:

S1. Experimental design of supplementary tests and discussion of results.

S2. Sources of variability.

Table S1. The schedule and conditions for each experimental run of primary experiments.

Table S2. The schedule and conditions for each experimental run of supplementary experiments.

Table S3. Fluorescence description for the eight categories of aerosol particles used to interpret WIBS data.

Table S4. Adjustment factors for the OPSs and the CO_2 meters based on side-by-side tests.

Figure S1. A comparison of deposition loss rate coefficients.

Figure S2. Asymmetry factors of total fluorescent aerosol particles generated in the supplementary experiments R37-R38.

Figure S3. Average count-weighted emission rates of total aerosol particles in the case of low RH conditions.

Figures S4-S5. Average count-weighted emission rates of total fluorescent aerosol particles in both high and low RH conditions.

Figures S6-S9. Average mass-weighted emission rates of total and fluorescent aerosol particles.

Figure S10. The variability of the count-weighted emission rates evaluated in cases without the use of moisturizer.

Figure S11. The skin hydration levels measured before and after acclimation.

Figure S12-S14. The influence of fluorescence threshold level on the average number-weighted emission rates of three primary particle fluorescence categories, respectively, for subject F1.

Figure S15-S20. Size distributions of number emissions of three primary particle fluorescence categories for the three subjects.

Figure S21. Count-weighted size distributions of nonfluorescent particle emissions for subject F1.

References

Adams, R.I., Bhangar, S., Pasut, W., Arens, E.A., Taylor, J.W., Lindow, S.E., Nazaroff, W.W. and Bruns, T.D. (2015) Chamber bioaerosol study: Outdoor air and human occupants as sources of indoor airborne microbes, *PLoS ONE*, **10**, e0128022.

Bhangar, S., Huffman, J.A. and Nazaroff, W.W. (2014) Size-resolved fluorescent biological aerosol particle concentrations and occupant emissions in a university classroom, *Indoor Air*, **24**, 604-617.

Bhangar, S., Adams, R.I., Pasut, W., Huffman, J.A., Arens, E.A., Taylor, J.W., Bruns, T.D. and Nazaroff, W.W. (2016) Chamber bioaerosol study: Human emissions of size-resolved fluorescent biological aerosol particles, *Indoor Air*, **26**, 193-206.

Cravello, B. and Ferri, A. (2008) Relationships between skin properties and environmental parameters, *Skin Res. Technol.*, **14**, 180-186.

Crawford, I., Robinson, N.H., Flynn, M.J., Foot, V.E., Gallagher, M.W., Huffman, J.A., Stanley, W.R. and Kaye, P.H. (2014) Characterisation of bioaerosol emissions from a Colorado pine forest: Results from the BEACHON-RoMBAS experiment, *Atmos. Chem. Phys.*, **14**, 8559-8578.

Crawford, I., Ruske, S., Topping, D.O. and Gallagher, M.W. (2015) Evaluation of hierarchical agglomerative cluster analysis methods for discrimination of primary biological aerosol, *Atmos. Meas. Tech.*, **8**, 4979-4991.

DMT. (2013) *Wideband Integrated Bioaerosol Spectrometer (WIBS-4A) Operator Manual DOC-0345 Revision A-2*. Droplet Measurement Technologies. Available online at: <http://www.dropletmeasurement.com/sites/default/files/ManualsGuides/Hardware%20Manuals/WIBS.pdf>.

Gabey, A.M., Gallagher, M.W., Whitehead, J., Dorsey, J.R., Kaye, P.H. and Stanley, W.R. (2010) Measurements and comparison of primary biological aerosol above and below a

tropical forest canopy using a dual channel fluorescence spectrometer, *Atmos. Chem. Phys.*, **10**, 4453-4466.
Gabey, A.M., Vaitilingom, M., Freney, E., Boulon, J., Sellegri, K., Gallagher, M.W., Crawford, I.P., Robinson, N.H., Stanley, W.R. and Kaye, P.H. (2013) Observations of fluorescent and biological aerosol at a high-altitude site in central France, *Atmos. Chem. Phys.*, **13**, 7415-7428.
Guirguis, O.W., Abd Elkader, M.F.H. and Nasrat, A.A. (2013) Enhancing antimicrobial activity for chitosan by adding jojoba liquid wax. *Mater. Lett.*, **93**, 353-355.
Hall, G.S., Mackintosh, C.A. and Hoffman, P.N. (1986) The dispersal of bacteria and skin scales from the body after showering and after application of a skin lotion, *J. Hyg. Cambridge*, **97**, 289-298.
Handorean, A., Robertson, C.E., Harris, J.K., Frank, D., Hull, N., Kotter, C., Stevens, M.J., Baumgardner, D., Pace, N.R. and Hernandez, M. (2015) Microbial aerosol liberation from soiled textiles isolated during routine residuals handling in a modern health care setting, *Microbiome*, **3**, 72.
Harding, C.R., Watkinson, A., Rawlings, A.V. and Scott, I.R. (2000) Dry skin, moisturization and corneodesmolysis, *Int. J. Cosmet. Sci.*, **22**, 21-52.
Healy, D.A., O'Connor, D.J. and Sodeau, J.R. (2012a) Measurement of the particle counting efficiency of the "Waveband Integrated Bioaerosol Sensor" model number 4 (WIBS-4), *J. Aerosol Sci.*, **47**, 94-99.
Healy, D.A., O'Connor, D.J., Burke, A.M. and Sodeau, J.R. (2012b) A laboratory assessment of the Waveband Integrated Bioaerosol Sensor (WIBS-4) using individual samples of pollen and fungal spore material, *Atmos. Environ.*, **60**, 534-543.
Healy, D.A., Huffman, J.A., O'Connor, D.J., Pöhlker, C., Pöschl, U. and Sodeau, J.R. (2014) Ambient measurements of biological aerosol particles near Killarney, Ireland: A comparison between real-time fluorescence and microscopy techniques, *Atmos. Chem. Phys.*, **14**, 8055-8069.
Hendriks, C.P. and Franklin, S.E. (2010) Influence of surface roughness, material and climate conditions on the friction of human skin, *Tribol. Lett.*, **37**, 361-373.
Hernandez, M., Perring, A.E., McCabe, K., Kok, G., Granger, G. and Baumgardner, D. (2016) Chamber catalogues of optical and fluorescent signatures distinguish bioaerosol classes, *Atmos. Meas. Tech.*, **9**, 3283-3292.
Hewitt, K.M., Gerba, C.P., Maxwell, S.L. and Kelley, S.T. (2012) Office space bacterial abundance and diversity in three metropolitan areas, *PLoS ONE*, **7**, e37849.
Hospodsky, D., Qian, J., Nazaroff, W.W., Yamamoto, N., Bibby, K., Rismani-Yazdi, H. and Peccia, J. (2012) Human occupancy as a source of indoor airborne bacteria, *PLoS ONE*, **7**, e34867.
Hospodsky, D., Yamamoto, N., Nazaroff, W.W., Miller, D., Gorthala, S. and Peccia, J. (2015) Characterizing airborne fungal and bacterial concentrations and emission rates in six occupied children's classrooms, *Indoor Air*, **25**, 641-652.
Huffman, J.A., Treutlein, B. and Pöschl, U. (2010) Fluorescent biological aerosol particle concentrations and size distributions measured with an Ultraviolet Aerodynamic Particle Sizer (UV-APS) in Central Europe, *Atmos. Chem. Phys.*, **10**, 3215-3233.
Jetté, M., Sidney, K. and Blümchen, G. (1990) Metabolic equivalents (METS) in exercise testing, exercise prescription, and evaluation of functional capacity, *Clin. Cardiol.*, **13**, 555-565.

Meadow, J.F., Altrichter, A.E., Kembel, S.W., Kline, J., Mhuireach, G., Moriyama, M., Northcutt, D., O'Connor, T.K., Womack, A.M., Brown, G.Z., Green, J.L. and Bohannan, B.J.M. (2014) Indoor airborne bacterial communities are influenced by ventilation, occupancy, and outdoor air source, *Indoor Air*, **24**, 41-48.

Meletiadis, J., Meis, J.F.G.M., Mouton, J.W. and Verweij, P.E. (2001) Analysis of growth characteristics of filamentous fungi in different nutrient media, *J. Clin. Microbiol.*, **39**, 478-484.

Mosteller, R.D. (1987) Simplified calculation of body-surface area, *New. Engl. J. Med.*, **317**, 1098.

Nazaroff, W.W. (2016) Indoor bioaerosol dynamics, *Indoor Air*, **26**, 61-78.

O'Connor, D.J., Daly, S.M. and Sodeau, J.R. (2015a) On-line monitoring of airborne bioaerosols released from a composting/green waste site, *Waste Manage.*, **42**, 23-30.

O'Connor, D.J., Healy, D.A. and Sodeau, J.R. (2015b) A 1-month online monitoring campaign of ambient fungal spore concentrations in the harbour region of Cork, Ireland, *Aerobiologia*, **31**, 295-314.

Pan, Y.L., Santarpia, J.L., Ratnesar-Shumate, S., Corson, E., Eshbaugh, J., Hill, S.C., Williamson, C.C., Coleman, M., Bare, C. and Kinahan, S. (2014) Effects of ozone and relative humidity on fluorescence spectra of octapeptide bioaerosol particles, *J. Quant. Spectrosc. Ra.*, **133**, 538-550.

Perring, A.E., Schwarz, J.P., Baumgardner, D., Hernandez, M.T., Spracklen, D.V., Heald, C.L., Gao, R.S., Kok, G., McMeeking, G.R., McQuaid, J.B. and Fahey, D.W. (2015) Airborne observations of regional variation in fluorescent aerosol across the United States, *J. Geophys. Res. Atmos.*, **120**, 1153-1170.

Pöhlker, C., Huffman, J.A. and Pöschl, U. (2012) Autofluorescence of atmospheric bioaerosols — fluorescent biomolecules and potential interferences, *Atmos. Meas. Tech.*, **5**, 37-71.

Qian, J., Hospodsky, D., Yamamoto, N., Nazaroff, W.W. and Peccia, J. (2012) Size-resolved emission rates of airborne bacteria and fungi in an occupied classroom, *Indoor Air*, **22**, 339-351.

Rawlings, A.V. and Harding, C.R. (2004) Moisturization and skin barrier function, *Dermatol. Ther.*, **17**, 43-48.

Shin, S.K., Kim, J., Ha, S.M., Oh, H.S., Chun, J., Sohn, J. and Yi, H. (2015) Metagenomic insights into the bioaerosols in the indoor and outdoor environments of childcare facilities, *PLoS ONE*, **10**, e0126960.

Su, S. and Guo, H. (2007) The association between low-humidity environment and skin dry symptoms among clean room workers, *Epidemiology*, **18**, S26.

Thatcher, T.L., Lai, A.C.K., Moreno-Jackson, R., Sextro, R.G. and Nazaroff, W.W. (2002) Effects of room furnishings and air speed on particle deposition rates indoors, *Atmos. Environ.*, **36**, 1811-1819.

Toprak, E. and Schnaiter, M. (2013) Fluorescent biological aerosol particles measured with the Waveband Integrated Bioaerosol Sensor WIBS-4: Laboratory tests combined with a one year field study, *Atmos. Chem. Phys.*, **13**, 225-243.

Veijgen, N.K., Masen, M.A. and van der Heide, E. (2013) Relating friction on the human skin to the hydration and temperature of the skin, *Tribol. Lett.*, **49**, 251-262.

Wang, L., Fan, D., Chen, W. and Terentjev, E.M. (2015) Bacterial growth, detachment and cell size control on polyethylene terephthalate surfaces, *Sci. Rep.*, **5**, 15159.

Whitehead, J.D., Gallagher, M.W., Dorsey, J.R., Robinson, N., Gabey, A.M., Coe, H., McFiggans, G., Flynn, M.J., Ryder, J., Nemitz, E. and Davies, F. (2010) Aerosol fluxes and dynamics within and above a tropical rainforest in South-East Asia, *Atmos. Chem. Phys.*, **10**, 9369-9382.

Wisniak, J. (1987) *The Chemistry and Technology of Jojoba Oil*, Champaign, Illinois, USA, American Oil Chemists' Society.

Wlodarski, M., Kaliszewski, M., Kwasny, M., Kopczynski, K., Zawadzki, Z., Mierczyk, Z., Mlynczak, J., Trafny, E. and Szpakowska, M. (2006) Fluorescence excitation-emission matrices of selected biological materials, *Proc. of SPIE*, **6398**, 639806.

Yamamoto, N., Hospodsky, D., Dannemiller, K.C., Nazaroff, W.W. and Peccia, J. (2015) Indoor emissions as a primary source of airborne allergenic fungal particles in classrooms, *Environ. Sci. Technol.*, **49**, 5098-5106.

Zhou, J., Chen, A., Cao, Q., Yang, B., Chang, V.W.C. and Nazaroff, W.W. (2015) Particle exposure during the 2013 haze in Singapore: Importance of the built environment, *Build. Environ.*, **93**, 14-23.